"Freezing-in" of Carbonylhemoglobin's CO Conformer Population by Hyperquenching of Its Aqueous Solution into the Glassy State: An FTIR Spectroscopic Study of the Limits of Cryofixation

Erwin Mayer

Contribution from the Institut für Allgemeine, Anorganische und Theoretische Chemie, Leopold-Franzens-Universität Innsbruck, A-6020 Innsbruck, Austria

Received January 26, 1994[⊗]

Abstract: Carbonylhemoglobin's (HbCO's) rapidly interconverting CO conformer bands are used as an indicator for the "limits of cryofixation". FTIR spectra of the CO stretching band region of HbCO in glassy aqueous solution obtained by hyperquenching at cooling rates of $\sim 10^6-10^7$ K s^{-1} and recorded at 78 K are compared with those of slow-cooled solutions, with either water or 75% (v/v) glycerol/water as solvent, which were recorded at several selected temperatures. The temperature dependence of the CIV/CIII conformer area ratios of HbCO in slow-cooled 75% glycerol/water solution is similar to that reported for the corresponding A_0/A_1 ratios in carbonylmyoglobin. For HbCO in slow-cooled aqueous solution, a further increase of the CIV/CIII area ratios in freeze-concentrated solution is attributed to dehydration of HbCO. For hyperquenched HbCO solution the percent relative band area of the curve-fitted component band due to conformer CIV is between the values of the slow-cooled aqueous solution recorded at 293 and 270 K, and according to this criterion, the conformer CIV population is "frozen-in" in this temperature range. The estimate of HbCO's conformer interconversion rate of $>10^4$ s^{-1}, or mean lifetime of $<10^{-4}$ s (Potter et al. *Biochemistry* **1990**, *29*, 6283−6295), gives an approximate value for the range of dynamic conformer equilibria which can be immobilized, or "frozen-in", close to ambient temperature by hyperquenching. It follows that the native state of biomolecules and its conformer population is better preserved in hyperquenched than in slow-cooled solution.

Introduction

It is common practice to cool solutions of biomolecules to cryogenic temperatures for further studies as diverse as follows: (i) study of the structure of a biomolecule by, e.g., resonance Raman spectroscopy,[1−10] (ii) study of the kinetics of ligand rebinding of, e.g., carbonylmyoglobin (MbCO) in glass-forming solution,[11−15] and (iii) cryoelectron microscopic study of the structure of a biomolecule.[16−23] For (i) and (ii), solutions are generally cooled at slow rates, and consequently, for conformationally inhomogeneous biomolecules whose conformers interconvert rapidly, the structure is *not* that present at ambient temperature, but it is that "frozen-in" at some low temperature. This is clearly seen for MbCO in 75% (v/v) glycerol/water solution where MbCO's A_0/A_1 conformer ratio increases by about an order of magnitude in going from ~280 to ~180 K, and is "frozen-in" on further cooling (read from Figure 4 in ref 12). A second example for the importance of structural changes on slow-cooling is given by Rousseau and Friedman[1] in their discussion of the possible origin of the difference between the room temperature and the cryogenic temperature behavior of the myoglobin photoproduct in terms of structural changes occurring during slow-cooling. For (iii), high cooling rates are considered to be of utmost importance, and for cryoelectron microscopic studies the aim of "cryofix-

[⊗] Abstract published in *Advance ACS Abstracts*, October 15, 1994.

(1) Reviewed by Rousseau, D. L.; Friedman, M. J. Resonance Raman Spectra of Heme and Metalloproteins. In *Biological Applications of Raman Spectroscopy*; Spiro, T. G., Ed.; Wiley: New York, 1988; Vol. 3, Chapter 4, pp 113−215.

(2) Ondrias, M. R.; Rousseau, D. L. *Science* **1981**, *213*, 657−659.

(3) Cho, K. C.; Rembda, R. D.; Fitchen, D. B. *Biochim. Biophys. Acta* **1981**, *668*, 186−192.

(4) Ondrias, M. R.; Rousseau, D. L.; Simon, S. R. *Proc. Natl. Acad. Sci. U.S.A.* **1982**, *79*, 1511−1514.

(5) Ondrias, M. R.; Rousseau, D. L. *J. Biol. Chem.* **1982**, *258*, 5638−5642.

(6) Czernuszewicz, R. S.; Johnson, M. K. *Appl. Spectrosc.* **1983**, *37*, 297−298.

(7) Bangcharoenpaurpong, O.; Schomaker, K. T.; Champion, P. M. *J. Am. Chem. Soc.* **1984**, *106*, 5688−5698.

(8) Rousseau, D. L.; Ondrias, M. R. *Biophys. J.* **1985**, *47*, 537−545.

(9) Sassaroli, M.; Dasgupta, S.; Rousseau, D. L. *J. Biol. Chem.* **1986**, *261*, 13704−13713.

(10) Reviewed by: Loehr, T. M.; Sanders-Loehr, J. *Methods Enzymol.* **1993**, *226*, 431−471.

(11) Ansari, A.; Berendzen, J.; Braunstein, D.; Cowen, B. R.; Frauenfelder, H.; Hong, M. K.; Iben, I. E. T.; Johnson, J. B.; Ormos, P.; Sauke, T. B.; Scholl, R.; Steinbach, P. J.; Vittitow, J.; Young, R. D. *Biophys. Chem.* **1987**, *26*, 337−355.

(12) Hong, M. K.; Braunstein, D.; Cowen, B.; Frauenfelder, H.; Iben, I. E. T.; Mourant, J. R.; Ormos, P.; Scholl, R.; Schulte, A.; Steinbach, P. J.; Xie, A.-H.; Young, R. D. *Biophys. J.* **1990**, *58*, 429−436.

(13) Srajer, V.; Reinisch, L.; Champion, P. M. *Biochemistry* **1991**, *30*, 4886−4895.

(14) Ansari, A.; Jones, C. M.; Henry, E. R.; Hofrichter, J.; Eaton, W. A. *Science* **1992**, *256*, 1796−1798.

(15) Doster, W.; Kleinert, Th.; Post, F.; Settles, M. In *Protein-Solvent Interactions*; Gregory, R. B., Ed.; Marcel Dekker: New York, 1993.

(16) Dubochet, J.; McDowall, A. W. *J. Microsc.* **1981**, *124*, RP3−RP4.

(17) Plattner, H.; Bachmann, L. *Int. Rev. Cytol.* **1982**, *79*, 237−304.

(18) Robards, A. W.; Sleytr, U. B. *Low Temperature Methods in Biological Electron Microscopy*; Elsevier: New York, 1985; Chapter 2.

(19) Bachmann, L.; Mayer, E. In *Cryotechniques in Biological Electron Microscopy*; Steinbrecht, R. A.; Zierold, K., Eds.; Springer-Verlag: Berlin, 1987; pp 1−34.

(20) Knoll, G.; Verkleij, A. J.; Plattner, H. In *Cryotechniques in Biological Electron Microscopy*; Steinbrecht, R. A.; Zierold, K., Eds.; Springer-Verlag: Berlin, 1987; pp 258−271.

(21) Sitte, H.; Edelmann, L.; Neumann, K. In *Cryotechniques in Biological Electron Microscopy*; Steinbrecht, R. A.; Zierold, K., Eds.; Springer-Verlag: Berlin, 1987; pp 87−113.

(22) Kellenberger, E. In *Cryotechniques in Biological Electron Microscopy*; Steinbrecht, R. A.; Zierold, K., Eds.; Springer-Verlag: Berlin, 1987; pp 35−63.

(23) Dubochet, J.; Adrian, M.; Chang, J.-J.; Homo, J. C.; Lepault, J.; McDowall, A. W.; Schultz, P. *Q. Rev. Biophys.* **1988**, *21*, 129−228.

0002-7863/94/1516-10571$04.50/0

ation" is to immobilize, or "freeze-in", the native state of dynamic structures and the momentary distribution of all components in a system.[17-23] But, for biological specimens, the spatial resolution of the electron microscope is below that necessary to see details on an atomic scale.[24]

Whether or not the conformer population at ambient temperature can be immobilized, or frozen-in, depends on the relative rates of cooling and of conformer interconversion and on their temperature dependencies. Apparently, the highest cooling rates are the best ones for immobilizing the structure and the conformer population of a biomolecule close to ambient temperature for subsequent further studies at cryogenic temperatures. These techniques were developed for vitrification of water and its dilute aqueous solutions[25,26] by so-called "hyperquenching" at estimated[19] and calculated[27] rates of $\sim 10^6$ to $\sim 10^7$ K s^{-1}, and were adapted for use in cryoelectron microscopy.[16,23] A first FTIR spectroscopic study of cryofixation of carbonylhemoglobin (HbCO) and metmyoglobin azide in aqueous solution had shown that the first can be immobilized but the second cannot.[28] The criterion was the amide I region of the first and the N−N stretching vibrations of the second.

In this study the CO stretching band region of HbCO is used as an indicator for changes in conformer population, and HbCO in glassy, or vitrified, aqueous solution made by hyperquenching is compared with HbCO in slow-cooled aqueous solution and in slow-cooled 75% (v/v) glycerol/water solution. The results are then discussed in a phenomenological context, by analyzing the CO stretching band parameters with respect to hyperquenching and slow-cooling, and they are further related to the behavior of MbCO in slow-cooled 75% glycerol/water solution reported by Frauenfelder and co-workers.[11,12]

Caughey and co-workers[29] have observed up to four discrete bands in the infrared spectra of solutions and crystals of HbCO, and have assigned those to discrete, rapidly interconverting conformers. For human HbCO, infrared peak positions for the four conformers are at 1932, 1943, 1951, and 1969 cm^{-1} which are designated as CI, CII, CIII, and CIV conformers, and similar peak positions are reported for most other HbCO's. ^{13}C NMR spectra support rapid interconversion among these four conformers, and the observation of only one NMR resonance has been interpreted by Potter et al.[29] in terms of a rate of interconversion among the conformers that is greater than the ^{13}C NMR time scale ($\sim 10^{-4}$ s).

The relative intensities of the four CO stretching bands, and therefore the relative population of the four conformers, depend among others on pH, temperature, and hydration of the protein. For HbCO the relative band areas, or conformer population, change sensitively with dehydration, and because of that HbCO is used in this study as an indicator for artifacts caused by dehydration in freeze-concentrated aqueous solution of biomolecules.[22,30] Brown et al.,[31] have reported that at 293 K for the hydration range 1.2−0.1 (g of water)/(g of HbCO) the relative area of the peak at ~ 1968 cm^{-1} (conformer CIV) increases with decreasing water content from 2.6% to 83% (read from Figure 4 in ref 31). The rate of increase with decreasing water content is much more pronounced for HbCO than for MbCO, and because of that HbCO was used as an indicator for dehydration artifacts although its bands contain overlapping contributions from both the α and β subunits of tetrameric HbCO.[29]

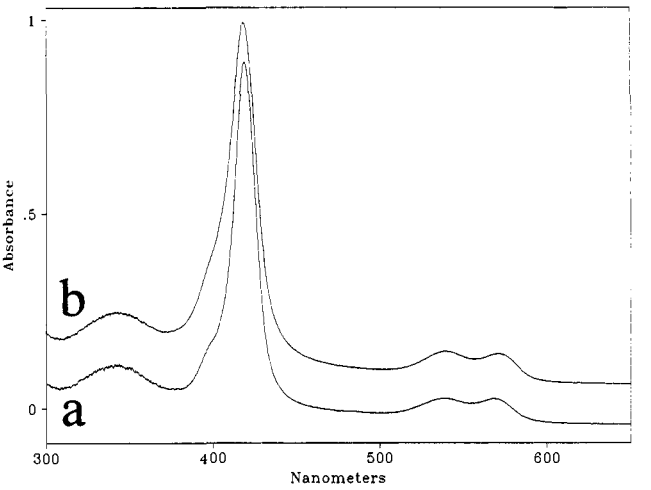

Figure 1. Absorption spectrum of HbCO in aqueous solution recorded at 295 K. (a) is the spectrum of the 1.2 mM stock solution, and (b) is that obtained after nebulizing the solution by ultrasonics and collecting the aerosol on a cold quartz disk.

Experimental Section

Bovine Hb was obtained from Fluka (No. 51290) and used as received. Aqueous HbCO solution was prepared by dissolving 0.50 g of Hb in 5.5 mL of 0.01 M potassium phosphate buffer solution, adding excess dithionite, and saturating the solution several times with CO (99.97%). A final pH of 6.8 at 293 K was obtained by adding sufficient basic buffer component. The solution was 1.2 mM, and quantitative conversion to HbCO was controlled in a UV−vis spectrophotometer.[33] For HbCO in 75% (v/v) glycerol/water solution, the same procedure was used, and the final pH at 293 K was 7.0. For studies of HbCO in slow-cooled aqueous solution it is important not to use sodium phosphate buffer salts because of drastic lowering of pH in freeze-concentrated solution.[34,35] This causes for HbCO, or MbCO, strongly enhanced intensity of the band at ~ 1968 cm^{-1} and can even lead to irreversible denaturation.[36]

The glassy, or vitrified, solution was prepared by so-called hyperquenching of aerosols on a CaF_2 window held at 78 K. Briefly, droplets of ~ 3 μm size made by means of an ultrasonic nebulizer (LKB Instruments, model 108, operating at 3 MHz) were suspended in N_2 gas and allowed to enter a high-vacuum cryostat though a 400 μm aperture. Once inside, the droplets moved toward the CaF_2 window at supersonic speeds and deposited on it. The intensity of the amide I spectral region was 0.5−1.5 absorbance units. In a separate experiment it was confirmed that the HbCO solution can be nebulized with our ultrasonic nebulizer without decomposition, and for that the UV−vis spectrum of the HbCO stock solution (a) is compared in Figure 1 with that obtained after nebulizing the solution, collecting the aerosol on a cold quartz disk, and recording its spectrum (b). Peak maxima and band shapes are identical in the two spectra except for the shoulder at ~400 nm which is better resolved in (a) than in (b). Aerosol formation by an ultrasonic nebulizer was preferred to that by a pneumatic nebulizer because with the first in our experience completely vitrified solutions are obtained for this solute concentration,[26,28,32] but with the second hyperquenched solutions contain still several percent crystalline ice, probably due to a small number of large droplets.[28] For further experimental details see refs 26, 28, and 32.

(24) Baumeister, W. *Ultramicroscopy* **1988**, *25*, 103−104.
(25) Brüggeller, P.; Mayer, E. *Nature* **1980**, *288*, 569−571. Mayer, E.; Brüggeller, P. *Nature* **1982**, *298*, 715−718.
(26) Mayer, E. *J. Appl. Phys.* **1985**, *58*, 663−667; *J. Microsc.* **1985**, *140*, 3−15; *Cryo-Lett.* **1988**, *9*, 66−77.
(27) Bald, W. B. *J. Microsc.* **1986**, *143*, 89−102.
(28) Mayer, E.; Astl, G. *Ultramicroscopy* **1992**, *45*, 185−197.
(29) Potter, W. T.; Hazzard, J. H.; Choc, M. G.; Tucker, M. P.; Caughey, W. S. *Biochemistry* **1990**, *29*, 6283−6295 and references therein.
(30) Kellenberger, E. *J. Microsc.* **1991**, *161*, 183−203.
(31) Brown III, W. E.; Sutcliffe, J. W.; Pulsinelli, P. D. *Biochemistry* **1983**, *22*, 2914−2923.
(32) Fleissner, G.; Hallbrucker, A.; Mayer, E. *J. Phys. Chem.* **1993**, *97*, 4806−4814.
(33) Waterman, M. R. *Methods Enzymol.* **1978**, *52*, 456−463.
(34) Van den Berg, L.; Rose, D. *Arch. Biochem. Biophys.* **1959**, *81*, 319−
(35) Murase, N.; Franks, F. *Biophys. Chem.* **1991**, *34*, 293−300.
(36) Astl, G.; Mayer, E. *Biochem. Biophys. Acta* **1991**, *1080*, 155−159.

Spectra of HbCO solution cooled slowly over hours in steps were obtained on cooling and reheating for the temperature range 293−78 K. Here the solution was held between two CaF_2 disks, and the sample thickness was ~7 μm. Crystallization of ice was observed at 260 K but not at 270 K. The rate of cooling or heating was between 2 and 5 K min^{-1}, and the sample was kept at each selected temperature for 5 min before recording its spectrum. Temperature was regulated in all experiments with the Paar controller model TTK-HC and was constant to ±0.1 K.

The FTIR spectra were recorded in transmission on Biorad's FTS 45 at 2 cm^{-1} resolution (UDR1), by coadding 256 scans. Water vapor was subtracted from the spectra, and for aqueous solutions the sloping background originating mainly from water's combination band was subtracted by the multipoint spline function routine provided by Biorad. For the spectral region used in this study, it is most important to avoid addition of small amounts of D_2O, as we had done in earlier studies to see clearly formation of crystalline ice via the decoupled OD stretching band,[28,32] because HOD contributes in this spectral region a broad band which makes subtraction of the sloping background very ambiguous. This band has not been noted before, but it is visible in some old spectra reported by Wyss and Falk.[37] For subtraction of the sloping background, break points were set at ≥2000 and ≤1915 cm^{-1}, after testing several other break point settings. The spectra were thereafter transferred to a PC and curve-fitted by using SpectraCalc's software. The band parameters obtained from the curve fits did not depend on the starting conditions of the curve-fitting procedure. The effects of baseline correction and of curve-fitting were further controlled first by comparing second-derivative curves of the original bands with those of the bands after subtraction of the sloping background, and second by comparing second derivatives of the background-corrected bands with those of the sum of the curve-fitted component bands. This comparison of second derivatives is in our experience a sensitive indicator for possible artifacts during manipulation of the data, and optimal superposition of second derivatives is taken as a criterion for the quality of the curve fits and of background subtraction.[38,39]

For background subtraction of the spectra of HbCO in 75% (v/v) glycerol/water solution, spectra of the solvent (containing identical amounts of potassium phosphate buffer) were obtained at identical temperatures, and these were then subtracted from those of the HbCO-containing solution.

Results

Figure 2 shows FTIR spectra of the CO stretching band region of HbCO in aqueous solution recorded at the given temperatures, with (a) being the original curves, but after subtraction of water vapor, and (b) those obtained after subtraction of the sloping background. The same stock solution was used for both hyperquenched and slow-cooled aqueous HbCO solution, with pH 6.8 at 293 K. Curves 1 are spectra of HbCO in glassy aqueous solution obtained by hyperquenching and recorded at 78 K, and curves 2−6 are spectra of a slow-cooled aqueous HbCO solution recorded at the given temperatures. In the slow-cooled solution, formation of ice started at 260 K, and curves 4−6 are those of a freeze-concentrated aqueous solution. Formation of ice is also made apparent in the original spectra by a change in the slope of the background due to water's combination band. The intensity of the band at ~1969 cm^{-1} due to conformer CIV is small, and similar, in curves 1−3, but in curves 4−6, which are for freeze-concentrated solution, it increases with decreasing temperature. During this experiment further spectra were recorded on both cooling and reheating which are not shown here but which are included in Figure 5c.

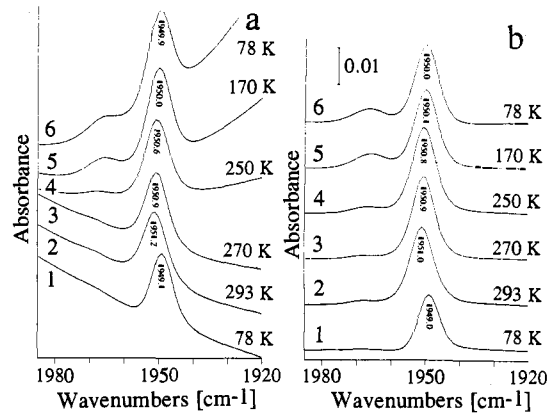

Figure 2. FTIR spectra of the CO stretching band region of 1.2 mM HbCO in aqueous solution. Curves 1 are for hyperquenched solution recorded at 78 K in the glassy state, and curves 2−6 are for slow-cooled solution recorded at the given temperatures. (a) are the original spectra, except for subtraction of water vapor, and (b) are the spectra after subtraction of the background with a multipoint spline function routine. The spectra of (b) are shown on the same scale but are shifted vertically for clarity.

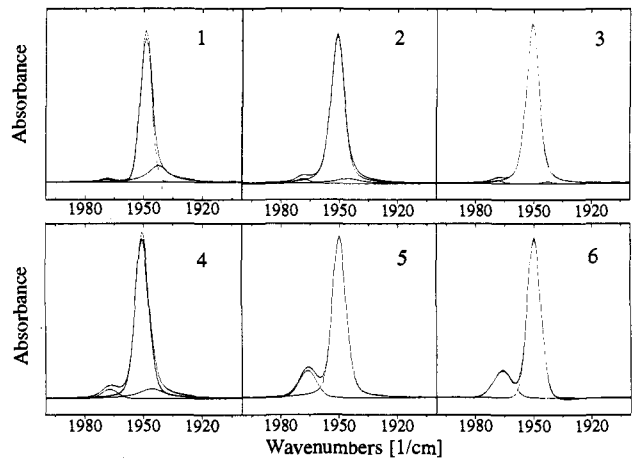

Figure 3. Curve fits of the spectra shown in Figure 1b. Curve 1 is the curve fit of the spectrum of HbCO in hyperquenched aqueous solution recorded at 78 K in the glassy state, and curves 2−6 are those of slow-cooled aqueous solution recorded at 293, 270, 250, 170, and 78 K, respectively.

Figure 3 shows curve fits of the six background-corrected spectra of Figure 2b. For spectra 1−4 three component bands were required for curve-fitting, and thus the conformer CI band at ~1932 cm^{-1} was not included in the curve fits because of its low intensity of only ~1%.[29] In freeze-concentrated aqueous solution the intensity of the band at ~1943 cm^{-1} due to conformer CII was observed to decrease from 250 to 210 K, and therefore for spectra 5 and 6 recorded at 170 and 78 K only two component bands were required for curve-fitting. Peak frequencies ($\tilde{\nu}_{max}$), full widths at half-height (fwhh), percent Gauss, and percent relative band areas of the curve-fitted component bands are listed in Table 1. The band parameters obtained for the CIII conformer at 293 and 270 K are nearly identical to those reported by Potter et al. for human HbCO at 301 and 277 K for pH 7.4, and the parameters of the other two bands are very similar (see Table 1 in ref 29).

The composite band shape of HbCO in hyperquenched and glassy solution is clearly more asymmetric at low frequency than those of HbCO solution recorded at 293 or 270 K. In curve fits using symmetrical band shapes, this asymmetry results

(37) Personal communication by M. Falk: see Wyss, H. R.; Falk, M. *Can. J. Chem.* **1970**, *48*, 607−614.
(38) Fleissner, G.; Hallbrucker, A.; Mayer, E. *Chem. Phys. Lett.* **1993**, *218*, 93−99.
(39) Gans, P. *Data fitting in the chemical sciences*; Wiley: New York, 1992; p 185.

Table 1. Curve-Fitting Analysis of HbCO's CO Stretching Band Region (from 1880 to 2020 cm^{-1}) for Hyperquenched Aqueous Solution in the Glassy State and for Slow-Cooled Aqueous Solution

sample	$\tilde{\nu}_{max}$ (cm^{-1})	fwhh (cm^{-1})	% Gauss	% relative area
(1) hyperquenched, 78 K	1969.0	7.2	100	1.6
	1949.0	6.9	100	77
	1942.5	11.9	0	21
(2) slow-cooled, 293 K	1968.8	7.4	100	2.2
	1951.1	8.1	53	91
	1945.3	14.3	0	6.5
(3) slow-cooled, 270 K	1968.8	6.7	100	1.4
	1950.7	7.9	58	98
	1942.8	5.4	100	0.7
(4) slow-cooled, 250 K	1967.5	9.7	100	5.1
	1950.7	8.0	68	83
	1946.0	15.9	0	11.9
(5) slow-cooled, 170 K	1966.4	10.7	100	16
	1950.1	8.2	64	84
(6) slow-cooled, 78 K	1966.3	11.6	90	20
	1950.1	8.2	100	80

for hyperquenched and glassy solution in a larger value for the relative band area of the band at ~1943 cm^{-1} at the expense of the 1951 cm^{-1} band than for the solution recorded at ambient temperature (Table 1). I can see the following explanations for this puzzling behavior: (i) enhanced intensity at low frequency is due to incorrect subtraction of the sloping background, (ii) intrinsic asymmetry of the band shape, (iii) asymmetry at low frequency is simply an artifact caused by the Christiansen effect due to scattering on the quenched water droplets,[40] and (iv) interconversion between conformers CII and CIII is more rapid than between CIV and CIII, and therefore, the CII and CIII conformer populations are frozen-in during hyperquenching at a much lower temperature than that of CIV. To exclude (i), several other background subtractions were investigated by shifting the break point at low frequency, which has been set at ≤1915 cm^{-1} for curve 1 of Figure 2b, to increasingly higher frequency. This obviously has the effect to reduce the relative area of the curve-fitted component band centered at ~1943 cm^{-1}. The quality of the curve fits obtained from these background-corrected spectra was then controlled by comparing the second derivative of the original composite band with that of the sum of the curve-fitted component bands. For break point settings of between ≤1915 and ≤1933 cm^{-1}, a comparison of second derivatives did not allow discrimination between the curve fits despite a decrease of the percent relative area of the component band at low frequency from 21% (Table 1) to 14% which is still higher than the values at ambient temperature (see Table 1). Only on further break point increase the error in background correction was clearly seen by comparison of second derivatives. However, for this range of background corrections which cannot be discriminated by comparison of second derivatives, the percent relative areas of conformers CIV and CIII vary only to a small extent, and from four curve fits the values are 1.5 ± 0.5% for the CIV conformer band area and 80 ± 3% for that of CIII. Since these values are the main topic of this study, the small spread is considered satisfactory. I conclude that the asymmetry at low frequency cannot be fully explained at present, and further experiments are planned to clarify this aspect.

In Figure 4a the FTIR spectrum of the CO stretching band region of HbCO in hyperquenched aqueous solution (curve 1) is compared with those of HbCO in slow-cooled 75% (v/v) glycerol/water solution (pH 7.0 at 293 K) recorded at the given temperatures (curves 2–6). For the spectra of HbCO in

(40) Mayer, E. *J. Phys. Chem.* **1985**, *89*, 3474–3477.

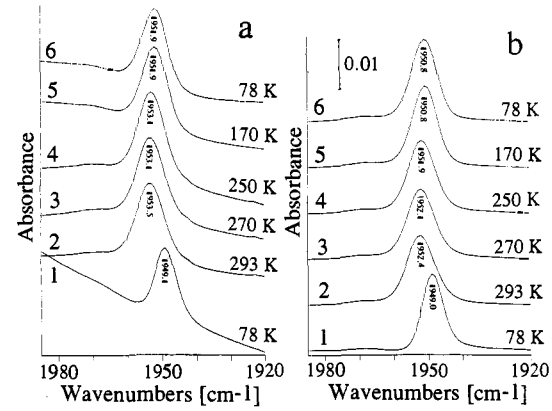

Figure 4. FTIR spectra of the CO stretching band region of 1.2 mM HbCO in slow-cooled 75% (v/v) glycerol/water solution (curves 2–6) recorded at the given temperatures, and their comparison with those of HbCO in hyperquenched aqueous solution recorded at 78 K in the glassy state. (a) are the original spectra, except for subtraction of water vapor, and (b) are the spectra after subtraction of solvent spectra recorded at the same temperature. The spectra of (b) are shown on the same scale but are shifted vertically for clarity.

Table 2. Curve-Fitting Analysis of HbCO's CO Stretching Band Region (from 1880 to 2020 cm^{-1}) for Hyperquenched Aqueous Solution in the Glassy State and for Slow-Cooled 75% (v/v) Glycerol/Water Solution

sample	$\tilde{\nu}_{max}$ (cm^{-1})	fwhh (cm^{-1})	% Gauss	% relative area
(1) hyperquenched, 78 K	1969.0	7.2	100	1.6
	1949.0	6.9	100	77
	1942.5	11.9	0	21
(2) slow-cooled, 293 K	1969.9	7.2	100	1.6
	1952.3	9.6	61	98
(3) slow-cooled, 270 K	1970.1	6.4	100	1.2
	1952.1	9.4	55	99
(4) slow-cooled, 250 K	1969.8	7.5	100	1.8
	1951.8	9.3	57	98
(5) slow-cooled, 170 K	1967.4	16.3	77	6.7
	1950.8	8.6	73	93
(6) slow-cooled, 78 K	1966.6	19.9	100	8.1
	1950.9	8.7	75	92

glycerol/water solution, subtraction of the background is more complicated, and less reliable, than for those of Figure 1a because glycerol contributes in this spectral region a weak broad band centered at ~1980–1985 cm^{-1}, with a fwhh of ~40 cm^{-1}, whose shape and peak position changes with temperature. This broad band extends into the CO stretching band region and thus cannot be subtracted with a multipoint spline function routine. Therefore, a set of HbCO-free solvent spectra was generated at the same temperatures, keeping all conditions as identical as possible. These were then subtracted from the spectra of the HbCO solution. For subtraction water's combination band was first used, and then subtraction was further optimized by aiming for a straight baseline above ~1990 cm^{-1} and below ~1920 cm^{-1}. This is similar to the technique recommended for the arduous subtraction of water's deformation band from the amide I spectral region of proteins.[41] For final correction of the background, a close-to-linear baseline, with break points ≥1995 and ≤1920 cm^{-1}, was subtracted. These spectra are shown in Figure 4b. Further spectra recorded during this experiment are included in Figure 5b.

Component band parameters of the curve fits of the spectra of Figure 4b are listed in Table 2. Only two component bands were included in the curve-fitting analysis because for the

(41) Dong, A.; Huang, P.; Caughey, W. S. *Biochemistry* **1990**, *29*, 3303–3308.

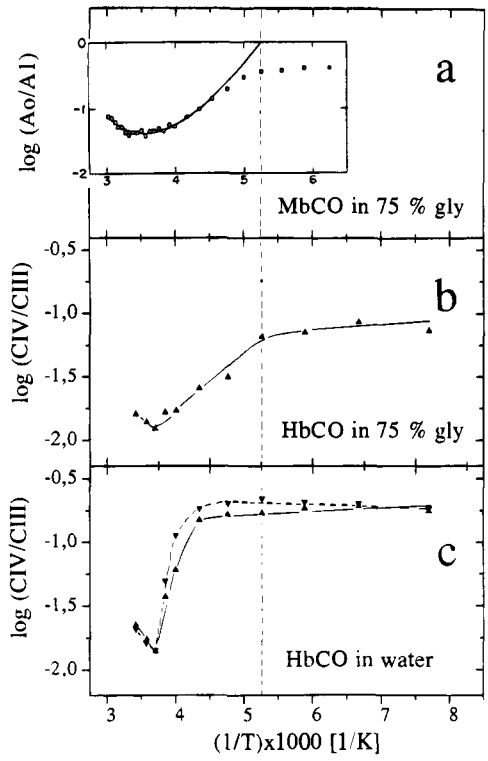

Figure 5. Log(conformer area ratios) versus $10^3/T$. (b) and (c) are for CIV/CIII area ratios of HbCO in 75% (v/v) glycerol/water solution and in water, respectively. (a) is the corresponding A_0/A_1 area ratio plot of MbCO in 75% (v/v) glycerol/water solution taken from Hong et al. (Figure 4b in ref 12). The vertical broken line is at 190 K. In (b) and (c), solid upright triangles are for data points obtained on cooling which are connected by solid lines to guide the eye. In (c), solid upside-down triangles are for data points obtained on reheating which are connected by the broken line.

spectrum recorded at 293 K, addition of a third component band invariably led during curve-fitting to unrealistic superposition of two curve-fitted bands at ~1950−1952 cm^{-1}. However, in the context of this study the important parameter is the percent relative area of the CIV component band as a function of temperature, and this band parameter shows for the spectra recorded between 270 and 78 K a very similar trend for curve fits with either two or three component bands.

In Figure 5 the log(conformer area ratios) of CIV/CIII recorded on slow cooling from 293 to 130 K are plotted versus $10^3/T$. (b) contains the log(area ratios) for HbCO in 75% glycerol/water solution and (c) the log(area ratios) for aqueous HbCO solution. In (a) the plot of log(area ratios) of the corresponding A_0/A_1 conformer bands of MbCO in 75% glycerol/water solution is shown for comparison from Figure 4b of Hong et al.[12] For (b) and (c), the values from Tables 1 and 2 are used, and further values are included which were obtained from spectra recorded during these experiments. Solid upright triangles are for data points obtained on cooling and are connected by solid lines to guide the eye, and in (c) solid upside-down triangles are for data points obtained on reheating and are connected by the broken line. Values recorded between 110 and 78 K are not shown here because this would give a distorted presentation of plot a, but these values continue the trend seen in (b) below 190 K and in (c) below 230 K. The vertical broken line is at 190 K, and it indicates the changes in slope for plots a and b. Note that for (a) 15 mM MbCO solution at pH 6.6 was used,[12] whereas for (b) and (c) the HbCO solution was 1.2 mM at pH 7.0 (b) and at pH 6.8 (c). The reduced scattering of the data points seen in (a) is probably due to the ~3-fold concentration of CO in the MbCO solution.

Discussion

Vandeginste and De Galan[42] have developed criteria for critical evaluation of curve-fitting in infrared spectroscopy (reviewed by Maddams, ref 43) which were extended by Gans and Gill[44] to infrared spectra of high signal-to-noise ratio. According to these criteria, artifact-free separation of a component band at ~1943 cm^{-1} (conformer CII) from that at ~1951 cm^{-1} (conformer CIII) by curve-fitting is not possible because separation of peak maxima is less than the half-bandwidth and intensities are too different. Nevertheless, the CII component bands have been included in the curve-fitting analysis of various forms of HbCO, and trends as a function of temperature or pH can give useful information.[29] However, for the component bands centered at ~1969 cm^{-1} (conformer CIV) and at ~1951 cm^{-1} (conformer CIII), separation of peak maxima is sufficient for reliable evaluation of the band parameters by curve-fitting. Therefore, in the following the emphasis is on the relative intensity of the CIV conformer, on CIV/CIII conformer area ratios, and on their temperature dependencies.

Slow-Cooled HbCO Solutions and the Comparison with MbCO. The four major conformational substates in both HbCO and MbCO, giving rise to up to four discrete CO stretching bands, are considered to have the same common origin. A molecular model recently developed by Oldfield et al.[45] attributed the observation of four major conformational substates in both HbCO and MbCO to electrical perturbation of the CO fundamental vibrational frequencies by distal histidine residues. In this model, interconversion between conformers CIV and CIII in HbCO, or A_0 and A_1 in MbCO, due to temperature, pressure, pH, and dehydration has been attributed to 180° ring flip isomerization of distal histidine residues. Therefore, comparison of the band parameters of slow-cooled HbCO solution and their temperature dependence with those of MbCO is possible and meaningful. Because of that, plots of log(CIV/CIII area ratios) versus $1/T$ are compared in Figure 5 for slow-cooled solution of HbCO in 75% (v/v) glycerol/water (b) and in water (c) with the corresponding plot of MbCO in 75% (v/v) glycerol/water solution taken from Hong et al.[12] (Figure 4b; conformers CIV and CIII in HbCO correspond to conformers A_0 and A_1 in MbCO).

Conformers CIV and CIII (or A_0 and A_1 in MbCO) have been specifically assigned to open and closed distal pocket conformational states, and the significance of conformer CIV (or A_0) in the dynamics of ligand entry-release processes and as a precursor to denaturation has been stressed.[11,12,29,31,45,46] The time scale for interconversion of conformers A_0 and A_1 in aqueous solution at 273 K is between ~1 and 10 μs.[46] Below a solvent's glass → liquid transition, or T_g, interconversion of conformers is stopped and the conformer population immobilized. For the popular 75% (v/v) glycerol/water solvent system this is below ~190 K, and it can be observed in plots of log(conformer area ratios) versus $1/T$ in the form of an abrupt change of slope toward a graph which becomes on further cooling nearly parallel to the abscissa.[11,12] Extrapolations from band areas to conformer populations presuppose identical, or very similar, integrated absorption coefficients. This is experimentally indicated for HbCO's bands at 1968 and 1951 cm^{-1}

(42) Vandeginste, B. G. M.; De Galan, L. *Anal. Chem.* **1975**, *47*, 2124−2132.
(43) Maddams, W. F. *Appl. Spectrosc.* **1980**, *34*, 245−267.
(44) Gans, P.; Gill, J. B. *Anal. Chem.* **1980**, *52*, 351−352.
(45) Oldfield, E.; Guo, K.; Augspurger, J. D.; Dykstra, C. E. *J. Am. Chem. Soc.* **1991**, *113*, 7537−7541.
(46) Tian, W. D.; Sage, J. T.; Champion, P. M. *J. Mol. Biol.* **1993**, *233*, 155−166.
(47) Choc, M. G.; Caughey, W. L. *J. Biol. Chem.* **1981**, *256*, 1831−1838.

(ref 47) and is used as a basic assumption for thermodynamic analysis of MbCO's CO stretching bands.[11,12]

In Figure 5 very similar behavior is observed for HbCO (b) and MbCO (a) in 75% glycerol/water solution: the CIV/CIII (A_0/A_1) conformer area ratio at first decreases upon cooling from ambient temperature to ~270 K and thereafter increases on further cooling. This surprising behavior has been analyzed in detail by Frauenfelder and co-workers[11,12] and is due to the temperature dependence of the protein's enthalpy and entropy (see ref 12 for further details). On further cooling an abrupt change of slope indicates for both HbCO and MbCO immobilization of conformer interconversion below the solvent's T_g at similar temperature. This behavior is not restricted to proteins, but has also been reported recently by Fishman et al.[48,49] for conformers of low molecular weight dissolved in glass-forming solution. For example, for pure 2-chlorobutane freezing-in of its rapidly interconverting conformers occurs on slow-cooling at ~97 K, but for 2-chlorobutane dissolved in Nujol exchange between its conformers stops already at ~205 K! The latter temperature correlates nicely with the calorimetric T_g of the solvent of ~210 K.[48,49]

In plot c where log(CIV/CIII area ratio) versus $1/T$ of HbCO in water is shown, the area ratio also first decreases on cooling from 293 to 270 K. For this temperature range the values for slow-cooled aqueous solution and the trend with temperature are consistent with the values reported by Potter et al. for human HbCO at similar pH values (compare Table 1 with Table 1 in ref 29).

On further cooling, the CIV/CIII area ratio also increases, but much more steeply and to a higher value than that of HbCO in 75% glycerol/water solution (b). (Note that for (b) and (c) the ordinates are drawn on the same scale to allow an estimate for this additional increase in aqueous solution.) The difference between plots b and c is due to the effects of formation of ice and subsequent freeze-concentration of the solute in c, and it is caused by increased relative intensity of the CIV conformer band which is at, e.g., 78 K 20% in slow-cooled aqueous solution but 8% in glycerol/water solution (see Tables 1 and 2). The effects of freeze-concentration can be dehydration of the solute, major shifts of pH, precipitation of salts, denaturation, and/or aggregation of proteins.[50] It appears that here dehydration is the primary effect of freeze-concentration, leading to enhanced population of the CIV conformer. This is consistent with Brown et al.'s[31] report of the influence of hydration on conformer population at 293 K. For plot c, CIV/CIII conformer area ratios are shown both on cooling as solid lines and on reheating as broken lines. The data points obtained on reheating first deviate from those obtained on cooling, and become identical only after melting of the ice. This is attributed to retarded crystallization during cooling. According to the CIV/CIII area ratio, the same state is obtained on reheating to 293 K, and therefore, irreversible aggregation and/or denaturation of HbCO can be excluded.

It has to be emphasized here that the steep increase in the CIV/CIII conformer area ratio in plot c is basically different from that shown in Figure 3 of ref 11 for MbCO in freeze-concentrated aqueous solution and explained there as slaved glass transition of the protein. This was subsequently shown to be caused by the "sodium phosphate buffer artifact" where in freeze-concentrated aqueous solution preferential precipitation of the basic buffer component leads to a drastic decrease in pH.[34-36] Decreasing pH also causes increasing population of conformer CIV and, as shown in ref 36, can lead even to irreversible denaturation of MbCO in freeze-concentrated solution. To avoid this artifact, potassium salts were used in this study instead of sodium salts, and furthermore, low concentrations were chosen deliberately to avoid precipitation.[35] According to plot c and Table 1, the relative area of conformer CIV increases on cooling to 78 K at most to ~20%. This also is clearly different from MbCO in freeze-concentrated and sodium phosphate buffered solution where immediately upon formation of ice at 260 K CIV develops into the dominant species (see Figure 3 in ref 11).

In plot c an abrupt change in slope on cooling toward a graph parallel to the abscissa occurs already at ~230 K whereas in plots b and a it is at ~190 K. This seems to indicate, in line with the argument given above, that conformer interconversion has stopped already below ~230 K on the time scale of the experiment and its population has been immobilized. It is well known that freeze-concentrated solutions formed upon precipitation of ice turn on further cooling into a glass,[50] and therefore, it cannot be excluded that interconversion of the conformers is stopped this way. However, studies of hydrated metHb and metMb powders by differential scanning calorimetry did not reveal any evidence for a sharp glass transitions,[51] such as that which can be observed in 75% glycerol/water solution and which causes the change in slope in plots a and b. It needs measurements which can probe directly the dynamics of conformer interconversion to determine if the abrupt change in slope in plot c is accidentally caused by the additional effect of HbCO's dehydration, or if it indicates immobilization of conformer interconversion.

Hyperquenching versus Slow-Cooling. Hyperquenching of a liquid at rates of ~10^6–10^7 K s^{-1} as done in this study produces a glass which has a higher enthalpy, entropy, and fictive temperature than a slow-cooled glass.[52] In general hyperquenched glasses are less dense than slow-cooled ones, but for dilute aqueous solutions where the density decreases with decreasing temperature in the supercooled state,[53] the opposite is to be expected. This is supported by the density of hyperquenched glassy water which is slightly higher than that of hexagonal ice at the same temperature.[54] It is important to note that the state of a hyperquenched glass differs from that of a slow-cooled glass both thermodynamically and kinetically.[52] Hyperquenched glasses, when kept at a temperature below their calorimetric glass transition, undergo exceptionally rapid relaxation of their structure by physical aging toward a state of lower enthalpy, entropy, and fictive temperature, thereby approaching the state of a slow-cooled glass.[52,55] The specific intention of this study is to determine, by comparison of the CIV/CIII conformer area ratio of HbCO in hyperquenched solution with those in slow-cooled solution, the temperature range where conformer interconversion is frozen-in during hyperquenching. This temperature range depends on the relative rates of cooling and conformer interconversion, and it can give an estimate for the limits of cryofixation.

In hyperquenched aqueous HbCO solution the relative area of the band at 1969 cm^{-1} is 1.5 ± 0.5%, and those of the aqueous solution recorded at 293 and 270 K are 2.1% and 1.4%

(48) Fishman, A. I.; Guseva, S. Yu.; Remizov, A. B.; Stolov, A. A.; Zgadzai, O. E. *Spectrochim. Acta* **1986**, *42A*, 1247–1253.
(49) Fishman, A. I.; Stolov, A. A.; Remizov, A. B. *Spectrochim. Acta* **1993**, *49A*, 1435–1479.
(50) Franks, F. In *Water, a Comprehensive Treatise*; Franks, F., Ed.; Plenum Press: New York, 1982; Vol. 7, pp 215–338.
(51) Sartor, G.; Mayer, E.; Johari, G. P. *Biophys. J.* **1994**, *66*, 249–258.
(52) Johari, G. P.; Hallbrucker, A.; Mayer, E. *J. Phys. Chem.* **1989**, *93*, 2648–2652.
(53) Angell, C. A. *In Water, a Comprehensive Treatise*; Franks, F., Ed.; Plenum Press: New York, 1982; Vol. 7, pp 1–81.
(54) Hofer, K.; Astl, G.; Mayer, E.; Johari, G. P. *J. Phys. Chem.* **1991**, *95*, 10777–10781 and ref 9 therein.
(55) Scherer, G. W. *Relaxation in Glass and Composites*; Wiley: New York, 1986.

(Table 1). Therefore, according to this criterion, the conformer CIV population is immobilized, or frozen-in, at a temperature between 293 and 270 K. These values depend somewhat on the method of background subtraction, as pointed out above, but the trend is the same. For human HbCO's conformer interconversion, a rate of $>10^4$ s^{-1}, or a mean lifetime of $<10^{-4}$ s, was estimated by Potter et al.[29] from ^{13}C NMR measurements at 293 K. This rate estimate gives an approximate lower-bound value for immobilization, or freezing-in, of conformer interconversion close to ambient temperature by hyperquenching. This estimate may have to be changed when the actual value of HbCO's conformer interconversion rate is determined more accurately in future studies.

The above-given estimate is consistent with another estimate where for a maximal experimentally accessible cooling rate of $\sim 10^7$ K s^{-1},[19,27] a "fixation time" of $\sim 10^{-5}$ s results by assuming that a temperature drop of $\sim$100 K is necessary for immobilizing the various motions.[19,28] This estimate neglects among others the temperature dependence of mean conformer lifetimes, but serves as a crude indicator for the limits of cryofixation. From this estimate of a fixation time it follows that dynamic conformer equilibria with mean lifetimes $\geq 10^{-5}$ s can be immobilized close to ambient temperature by hyperquenching whereas dynamic equilibria with shorter mean lifetimes can be immobilized even by hyperquenching only at increasingly lower temperatures. An example for the latter is the high-spin/low-spin equilibrium in metmyoglobin azide.[28] It is important to note that this estimate of a fixation time is also consistent with Tian et al.'s[46] value for the time scale of interconversion of A_0 and A_1 conformers at 273 K which is up to $\sim 10^{-5}$ s.

The value of the peak frequency of the CIII conformer centered in hyperquenched solution at 1949.0 cm^{-1} requires further discussion. This value is clearly below those of the slow-cooled solutions, and since this band parameter is probably the most accurate one, this is considered significant. The peak frequency of the CIII conformer decreases on going from 293 to 78 K in slow-cooled aqueous solution from 1951.1 to 1950.1 cm^{-1} by 1.0 cm^{-1} (Table 1) and in 75% glycerol/water solution from 1952.3 to 1950.9 cm^{-1} by 1.4 cm^{-1} (Table 2). Therefore, HbCO in hyperquenched solution corresponds, with respect to its peak frequency of the CIII conformer band, to a state which is not accessible by slow-cooling. This also follows by considering that the hyperquenched glass kept at, e.g., 78 K is expected to have a density which differs from that of a slow-cooled glass at the same temperature.[53]

The effect of temperature on the value of a stretching frequency is not trivial. For example, Sceats and Rice[56] have attributed the increase in frequencies of the uncoupled OH and OD oscillators in hexagonal ice with increasing temperature to thermal expansion. This temperature dependence at constant pressure can be further separated into a contribution of temperature at constant volume and a volume effect at constant temperature, by investigating both the temperature and pressure dependence of the in-phase O−H stretching vibration. This has been done by Sivakumar et al.[57] for hexagonal ice, and the contributions have been analyzed and attributed to the various possible effects, but even in this detailed study unambiguous assignment was not possible. For MbCO or HbCO these values are not known. It is important to note that for MbCO in 75% glycerol/water solution the opposite temperature dependence has been reported, i.e., *increasing* peak frequency of the A_1 conformer band with decreasing temperature (see Figure 8 in ref 11). These differences are not understood, but they apparently are related to subtle differences in perturbation of the heme−CO ligand and their temperature dependencies.

The difference in the behavior of conformer distribution and peak frequencies can be further understood by considering the changes occurring during hyperquenching. When a liquid is subjected to a sudden change in temperature (or pressure), its properties exhibit a nearly instantaneous, solidlike, elastic change. This is followed by a slower, liquidlike structural relaxation to new equilibrium values at the new temperature (or pressure).[58] During hyperquenching of a liquid into the glassy state, the elastic change cannot be prevented, but the second can because the time scale for structural relaxation increases rapidly with decreasing temperature until below the glass transition region it is kinetically arrested.[58] In this study the structural change investigated is the change in the CO conformer population with temperature, and cryofixation of the CO conformer population requires, as pointed out above, that the fixation time is shorter than the mean conformer lifetime at ambient temperature. However, changes in peak frequency during hyperquenching can be instantaneous, and therefore cannot be prevented even by extreme rates of cooling. It is important to note that in pressure-release relaxation experiments fast changes in peak frequencies of the A conformer bands of MbCO in 75% glycerol/water solution have been interpreted as an elastic relaxation.[59] Simulation of a cooling process of proteins by molecular dynamics indicates that cooling leads to a contraction of the protein's structure.[60] One of the many effects which could lower the peak frequency of conformer CIII in hyperquenched solution below the value of slow-cooled solution is increased anharmonicity of the vibrational mode in the densified structure of the hyperquenched protein.

Nonequilibrium distributions of conformers can be generated in particular by a pressure jump or a temperature jump for studying subsequent structural relaxation toward equilibrium.[58,59,61] The first was used extensively by Frauenfelder and co-workers[59,61] to study MbCO's conformational relaxation. The second approach was used by Ansari et al. for MbCO in 75% glycerol/water solution, and by clever choice of the temperature region even slow cooling by 5° was sufficient to generate a nonequilibrium distribution and to follow isothermally the approach of conformer A_0 toward equilibrium (see Figure 10 in ref 11). Hyperquenching of glassy solutions of HbCO, and also of MbCO, into the glassy state produces an extreme nonequilibrium conformer distribution. Its approach to equilibrium as a function of temperature and/or time can now be studied conveniently. This is better done with hyperquenched glycerol/water solution to avoid complications by formation of ice.

Acknowledgment. I am grateful for financial support by the Forschungsförderungsfonds of Austria (Project No. P10404-PHY) and to our group for patient help and discussions.

(56) Sceats, M. G.; Rice, S. A. In *Water, a Comprehensive Treatise*; Franks, F., Ed.; Plenum Press: New York, 1982; Vol. 7, pp 83−214.

(57) Sivakumar, T. C.; Chew, H. A. M.; Johari, G. P. *Nature* **1978**, *275*, 524−525.

(58) Moynihan, C. T.; Macedo, P. B.; Montrose, C. J.; Gupta, P. K.; DeBolt, M. A.; Dill, J. F.; Dom, B. E.; Drake, P. W.; Easteal, A. J.; Elterman, P. B.; Moeller, R. P.; Sasabe, H.; Wilder, J. A. *Ann. N. Y. Acad. Sci.* **1976**, *279*, 15−36.

(59) Iben, I. E. T.; Braunstein, D.; Doster, W.; Frauenfelder, H.; Hong, M. K.; Johnson, J. B.; Luck, S.; Ormos, P.; Schulte, A.; Steinbach, P. C.; Xie, A. H.; Young, R. D. *Phys. Rev. Lett.* **1989**, *62*, 1916−1919.

(60) Tesch, M.; Schulten, K. *Chem. Phys. Lett.* **1990**, *169*, 97−102.

(61) Frauenfelder, H.; Alberding, N. A.; Ansari, A.; Braunstein, D.; Cowen, B. R.; Hong, M. K.; Iben, I. E. T.; Johnson, J. B.; Luck, S.; Marden, M. C.; Mourant, J. R.; Ormos, P.; Reinisch, L.; Scholl, R.; Schulte, A.; Shyamsunder, E.; Sorensen, L. B.; Steinbach, P. J.; Xie, A.; Young, R. D.; Yue, K. T. *J. Phys. Chem.* **1990**, *94*, 1024−1037.